Orientation Control of High-χ Triblock Copolymer for Sub-10 nm Patterning Using Fluorine-Containing Polymeric Additives

Jiajing Li[a], Chun Zhou[a], Xuanxuan Chen[a], Paulina A. Rincon-Delgadillo[b], Paul F. Nealey[a,c*]

[a]Institute for Molecular Engineering, University of Chicago, Chicago, IL 60637 USA
[b]IMEC, Kapeldreef 75, Heverlee, 3001 Belgium
[c]Material Science Division, Argonne National Laboratory, Lemont, IL 60439, USA

Abstract. Directed self-assembly (DSA) of block copolymers (BCPs) is one of the most promising techniques to tackle the ever-increasing demand for sub-lithographic features in semiconductor industries. BCPs with high Flory Huggins parameter (χ) are of particular interest due to their ability to self-assemble at the length scale of sub-10 nm. However, such high-χ BCPs typically have imbalanced surface energies between respective blocks, making it a challenge to achieve desired perpendicular orientation. To address this challenge, we mixed a fluorine-containing polymeric additive with poly(2-vinylpyridine)-*block*-polystyrene-*block*-poly(2-vinylpyridine) (P2VP-*b*-PS-*b*-P2VP) and successfully controlled the orientation of the high-χ triblock copolymer. The additive selectively mixes with P2VP block through hydrogen bonding and can reduce the dissimilarity of surface energies between PS and P2VP blocks. After optimizing additive dose and annealing conditions, desired perpendicular orientation formed upon simple thermal annealing. We further demonstrated DSA of this material system with 5 times density multiplication and a half pitch as small as 8.5 nm. This material system is also amenable to sequential infiltration synthesis treatment to selectively grow metal oxide in P2VP domains, which can facilitate the subsequent pattern transfer. We believe that this integration-friendly DSA platform using simple thermal annealing holds the great potential for sub-10 nm nanopatterning applications.

Key words: directed self-assembly, block copolymer, lithography, sub-10 nm, sequential infiltration synthesis

*Paul F. Nealey, E-mail: nealey@uchicago.edu

1 Introduction

The linear dimensions of transistors have been reduced by half every three years during the past five decades, which was mainly accomplished by reducing the wavelength of light used in lithography. Current state-of-the-art immersion photolithography tools using deep ultraviolet light with wavelength of 193 nm can reach 40 nm resolution limit with a single exposure. However, when the wavelength further goes down to the extreme ultraviolet at 13.5 nm, considerable challenges are faced such as the tool cost, uptime and stochastic variations. As an alternative technique for ultra-high resolution patterning, directed self-assembly (DSA) has attracted great academic and industrial interest since it was first introduced over a decade ago[1].

37 DSA is a patterning technique that orders the self-assembling block copolymers (BCPs) using
38 a chemical or topological template. The assembly of BCPs is well guided by the template, and
39 the resulted structures resemble critical features in integrated circuits such as line/space and
40 contact holes. DSA is especially attractive due to its ability to multiply the density of
41 lithographical features on the template, denoted as density multiplication, which can extend
42 optical lithography far beyond its current limits[2]. Polystyrene-*b*-poly(methyl methacrylate)
43 (PS-*b*-PMMA) is the most widely studied BCP for DSA applications because of the similar
44 surface energies of PS and PMMA blocks, which enables desired perpendicular orientation by
45 thermal annealing with a free surface. DSA of PS-*b*-PMMA with 14 nm half pitch line/space
46 pattern has been implemented on 300 mm wafer processing line at IMEC with relatively low
47 defect density, approaching that required for high volume manufacturing[3]. However, PS-*b*-
48 PMMA has a resolution limit of 11 nm due to its low Flory−Huggins interaction parameter (χ),
49 which prevents microphase separation and pattern transfer at smaller pitch. As a result, it is
50 imperative to explore more BCPs with higher χ in order to achieve the desired sub-10 nm
51 feature size.

52 One promising high-χ BCP is poly(2-vinyl-pyridine)-*block*-polystyrene-*block*-poly(2-vinyl-
53 pyridine) (P2VP-*b*-PS-*b*-P2VP) with χ equal to 0.10 at 200°C compared with 0.037 for that of
54 PS-*b*-PMMA[4]. Though higher χ enables P2VP-*b*-PS-*b*-P2VP (VSV) to microphase separate
55 into lamellar structures at sub-10 nm feature size, forming perpendicularly oriented BCP
56 domains remains a challenge due to imbalanced surface energies of PS and P2VP blocks[5]. The
57 surface tension of PS is 40.7 mN/m and that of P2VP is 49.4 mN/m[6], resulting in undesired
58 parallel orientation upon annealing. Several approaches have been developed to circumvent the
59 problem of dissimilar surface energies, including solvent vapor annealing[7], vapor-phase
60 deposited top coat[8] and embedded neutral layer[9]. Despite the successful orientation control
61 these approaches have achieved, challenges still remain to meet all the requirements for large

62 scale manufacturing. For example, there is no solvent annealing tool currently available for
63 manufacturing, and top coat approaches require additional processing steps, which lead to
64 increased complexity and costs. The segregated neutral layer topcoat also brings challenges for
65 pattern transfer by dry etching.

66 Our strategy to control the orientation of VSV is to use a fluorine-containing polymeric additive
67 poly(hexafluoroalcohol styrene) (PHFAS), which enables perpendicular orientation of VSV by
68 simple thermal annealing. The same polymeric additive has been shown to effectively tune the
69 surface energies of other block copolymers[10]. PHFAS has lower surface energy than both PS
70 and P2VP blocks, and it can selectively interact with P2VP via hydrogen bonding to lower the
71 apparent surface energy of P2VP block. By carefully adjusting the amount of PHFAS in the
72 system, the surface energies of PS and P2VP blocks can be balanced and desired perpendicular
73 orientation can form upon thermal annealing. After optimizing PHFAS dose and annealing
74 conditions, we further demonstrate DSA of VSV/PHFAS with density multiplication on
75 chemical patterns. We also investigate the pattern transfer potential of this material system
76 assisted by sequential infiltration synthesis (SIS). Finally, we discuss the impact of molecular
77 weight of PHFAS on orientation control and offer a simple yet effective way to predict the
78 molecular weight of PHFAS needed for a given VSV.

79 **2 Experimental**

80 *2.1 Materials*

81 VSV with three different molecular weights (M_n=26 kg·mol^{-1}, 33 kg·mol^{-1} and 47 kg·mol^{-1})
82 were purchased from Polymer Source, Inc. PHFAS additives with two molecular weights
83 (M_n=4.4 kg·mol^{-1}, M_w=5.9 kg·mol^{-1}; M_n=6.7 kg·mol^{-1}, M_w=9.5 kg·mol^{-1}) were synthesized via
84 free radical polymerization as described elsewhere[10]. Hydroxyl-terminated polystyrene-
85 *random*-poly(2-vinyl-pyridine) (PS-*r*-P2VP-OH) was synthesized in our group as previously

reported[11]. Silicon <100> wafers were purchased from WRS Materials, LLC. All solvents were purchased from Aldrich and used as received.

2.2 Self-assembly of VSV with PHFAS additive

A solution of 1.5 wt% PS-*r*-P2VP-OH in dimethylformamide (DMF) was spin coated on clean silicon wafers followed by annealing at 200°C for 10 min under a nitrogen atmosphere. The brush was grafted on surface via reaction between hydroxyl group at the chain end and the silicon oxide surface. Ungrafted polymer brush was removed by sonication in DMF and the substrates were dried with nitrogen. The thickness of grafted brush was approximately 8 nm. Brush modified wafers were then coated with 1 wt% VSV/PHFAS solution in DMF and annealed under a nitrogen atmosphere. The thickness of VSV/PHFAS film after annealing was approximately 20 nm.

2.3 Directed self-assembly of VSV with PHFAS additive

The DSA process was adapted from previously reported process[12]. Briefly, silicon wafers were spin coated with cross-linkable polystyrene solution and annealed at 250°C for 5 min under a nitrogen atmosphere to drive the crosslinking reaction. Chemical patterns were prepared using electron-beam lithography followed by exposure to oxygen plasma, which trimmed the crosslinked polystyrene (xPS) guiding stipes to the desired width. After oxygen plasma, the excess resist was removed by repeated sonication in N-methyl-2-pyrrolidone and chlorobenzene. Alternatively, silicon wafers with xPS guiding stripes were also received from IMEC prepared by a previously reported approach[13]. PS-*r*-P2VP-OH brush was then grafted onto the wafers and VSV film with optimized PHFAS dose was annealed under a nitrogen atmosphere.

3 Results and discussion

109 *3.1 Orientation control of VSV with PHFAS additive*

110 In order to achieve desired perpendicular orientation, both interfacial energies between
111 substrate and BCP as well as surface energies between BCP and nitrogen atmosphere need to
112 be balanced. Interfacial energies can be readily tuned by employing random copolymer brush
113 with optimized PS content, which is non-preferential to respective blocks[11]. For VSV, however,
114 surface energies are not balanced since surface energy of PS is lower than that of P2VP. To
115 reduce this dissimilarity, we introduce PHFAS as a surface energy balancer to lower the
116 apparent surface energy of P2VP block.

117 We first investigate two possible factors that might affect to the orientation control of VSV:
118 PHFAS dose and annealing temperatures. We start with a relatively large VSV (47 kg·mol^{-1})
119 to optimize these factors following the schematic in Fig. 1a. The substrate is modified with PS-
120 *r*-P2VP-OH brush containing 48% PS, which has been identified non-preferential to VSV[11].
121 VSV solutions with various doses of PHFAS (M_w=9.5 kg·mol^{-1}) are spin-coated on brush
122 modified substrates and annealed under nitrogen atmosphere at different temperatures.

123 When PHFAS dose is low (below 6 wt%), parallel lamellae are the predominant structures due
124 to imbalanced surface energies (Fig. 1b). PS block is more favored by the top surface than
125 P2VP block due to its lower surface energy. As PHFAS dose increases, perpendicular
126 orientation begins to form as a result of more balanced surface energies. When PHFAS dose
127 reaches 12 wt% (with respect to VSV), full perpendicular orientation can be observed at 200°C.
128 PHFAS is expected to stay in the P2VP block via the hydrogen bonding, and is likely to
129 aggregate on top of the P2VP block during annealing because of its lower surface energy.
130 Periodicity (L_0) of the self-assembled pattern is 23.0 nm as measured by Fast Fourier Transform
131 (FFT) analysis of the top-down SEM images. It is worth noting that L_0 increases by
132 approximately 7.5% compared with that from solvent annealing[14], which can be attributed to
133 two possible reasons. It is likely that the effective χ of VSV increases with the presence of

134 PHFAS[15], which can potentially lead to larger L_0 and lower line edge roughness. In this case,
135 PHFAS is most likely only distributed in the P2VP block as we hypothesized. If PHFAS is
136 equally distributed in both blocks, χ should decrease rather than increase. Alternatively, it is
137 also possible that the presence of PHFAS can affect the chain conformations of P2VP block
138 and thus increase L_0.

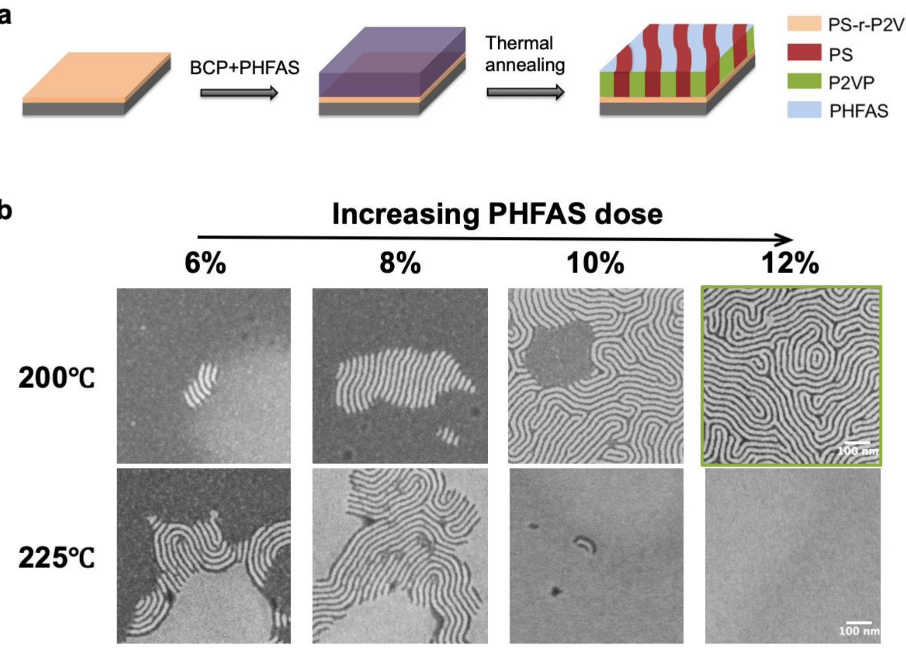

139

140 **Fig. 1** (a) Process flow for self-assembly of VSV with PHFAS additive. (b) SEM images of VSV with various
141 doses of PHFAS upon thermal annealing on neutral substrates. Brighter domain is P2VP and darker domain is PS.
142 Full perpendicular orientation forms with 12% PHFAS at 200 °C. L_0 is 23.0 nm as measured from FFT analysis.

143 *3.2 Directed self-assembly of VSV with PHFAS additive*

144 The self-assembly of lamellae-forming BCPs can be directed using chemically contrast
145 patterns comprising of guiding stripes of cross-linked homopolymer mat and interspatial
146 random copolymer brush[16], which is usually denoted as chemo-epitaxy DSA. The key to
147 chemo-epitaxy DSA is the ability of BCPs to recognize the chemical patterns and align
148 along the guiding stripes based on the wetting preference. It is crucial that VSV still
149 preserves this ability when mixed with PHFAS.

150 The chemo-epitaxy DSA of VSV/PHFAS with 3 times density multiplication is
151 demonstrated following the schematic shown in Fig. 2a. The substrate is coated with xPS
152 followed by E-beam lithography. After removing xPS in the exposed areas and trim etching
153 the xPS guiding stripes underneath E-beam resist lines with oxygen plasma, the E-beam
154 resist is stripped and the exposed areas between xPS guiding lines are subsequently
155 backfilled with the same neutral PS-*r*-P2VP-OH brush used in Fig. 1. VSV (47k) with 12%
156 PHFAS (9.5k) is spin-coated on chemical patterns and annealed at 200℃. Successful DSA
157 with 23 nm full pitch (Fig. 2c) is demonstrated on a template with the initial pitch L_s=69
158 nm (Fig. 2b). This confirms that the presence of PHFAS does not impair the ability of VSV
159 to recognize the chemical contrast of the chemical patterns and thus the standard chemo-
160 epitaxy DSA scheme is still valid.

161 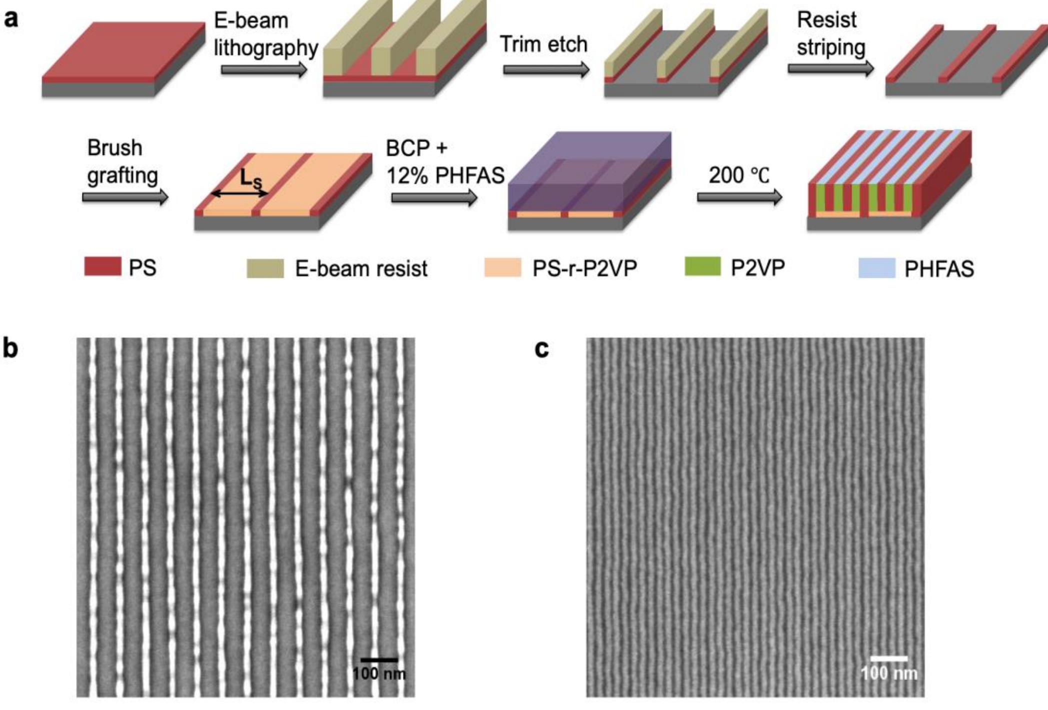

162 **Fig. 2** (a) Process flow for chemo-epitaxy DSA of VSV with PHFAS additive. (b) SEM image of the template
163 after trim etch and (c) DSA pattern with 23.0 nm full pitch after assembly.

164 *3.3 Mask conversion of BCP pattern with SIS*

165 In order to implement the DSA line/space patterns for advanced patterning applications, the
166 patterns need to be transferred from the BCP films to the underlying substrates, which desires
167 high etching contrast between different blocks of the BCP. One effective way to increase the
168 etching contrast of VSV is SIS, where metal oxide such as alumina selectively infiltrates the
169 P2VP block while PS block is relatively unaffected. VSV is then removed by oxygen plasma,
170 leaving the alumina lines mimicking the original patterns of P2VP blocks which afterwards
171 could be used as effective etching masks[17]. The alumina mask is more resistant to a variety of
172 etching chemistries compared with the original soft matter films and thus could facilitate the
173 direct pattern transfer to the underlying substrates without the need of an additional hard mask
174 layer[7,8]. Our group has previously demonstrated pattern transfer of VSV to silicon substrates
175 with 8 nm half pitch using this technique[7].

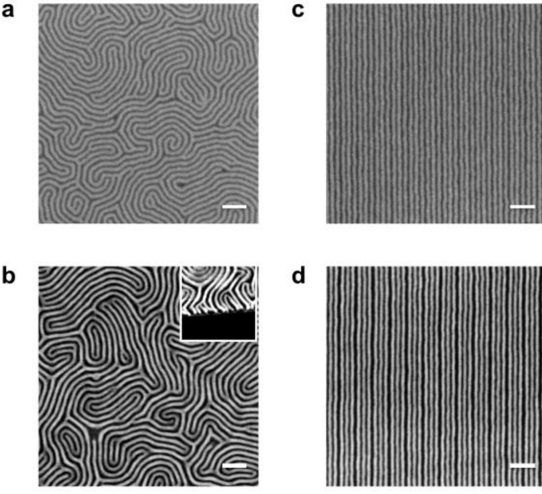

176

177 **Fig. 3** SEM images of assembled VSV (a, b) after SIS and (c, d) after oxygen plasma on neutral substrates and on
178 chemical patterns. Scale bars represent 100 nm.

179 As PHFAS is also expected to form hydrogen bonding with the precursors of SIS, it is critical
180 that the presence of PHFAS does not interfere with the SIS process. Fig. 3 shows self-assembly
181 pattern and DSA pattern of VSV/PHFAS after three cycles of SIS (Fig. 3a, 3c) and after
182 polymer removal by oxygen plasma (Fig. 3b, 3d). The clear trenches after polymer removal
183 indicate that no alumina has formed in PS domains, and no wetting layer has formed on top or
184 at bottom of the film. This confirms that the presence of PHFAS does not affect SIS or bring

185 extra complexities to the pattern transfer process compared with pure VSV. Though pitch
186 walking has been observed after polymer removal of the DSA pattern, it mainly comes from
187 the DSA and pattern transfer process rather than the PHFAS, which can be improved by further
188 optimizing the process such as using short PS brush[7] or adjusting the depth of alumina
189 infiltration.

190 *3.4 Effect of molecular weight of PHFAS on orientation control*

191 We have shown that PHFAS can effectively control the orientation of VSV (47k) and achieved
192 DSA line/space pattern with 23 nm full pitch. In order to apply the same strategy to smaller
193 VSV for sub-10 nm patterning, we investigate the effect of molecular weight of PHFAS on
194 orientation control. We use VSV with three molecular weights (26k, 33k and 47k) and PHFAS
195 with two molecular weights (5.9k and 9.5k).

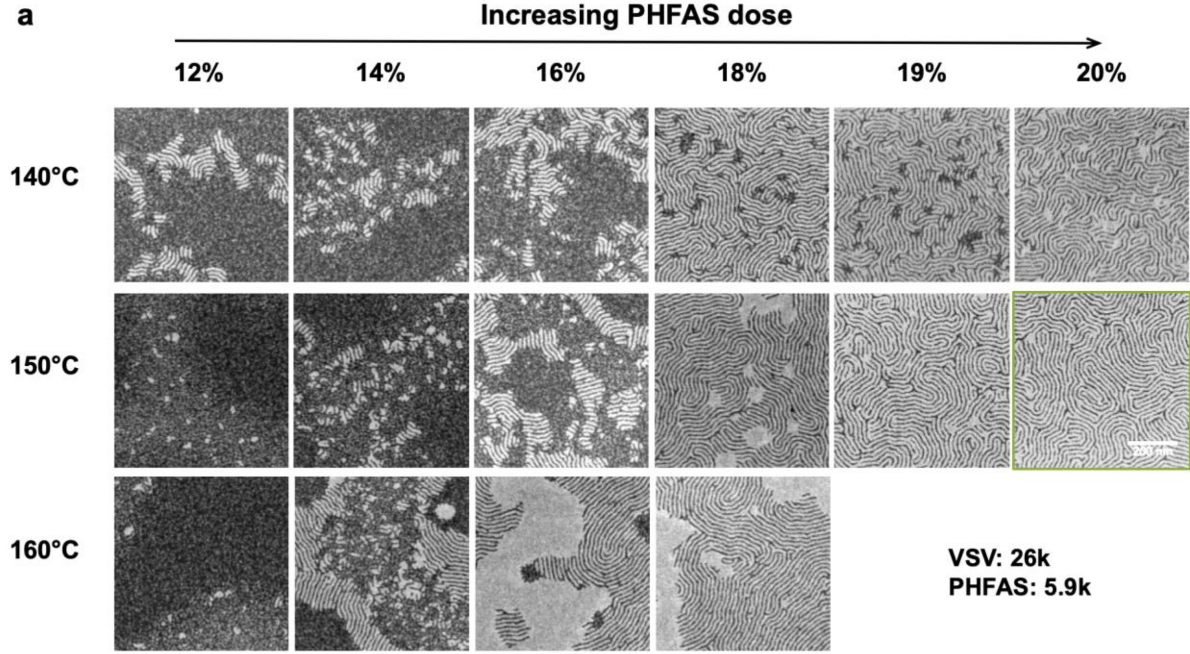

196

197

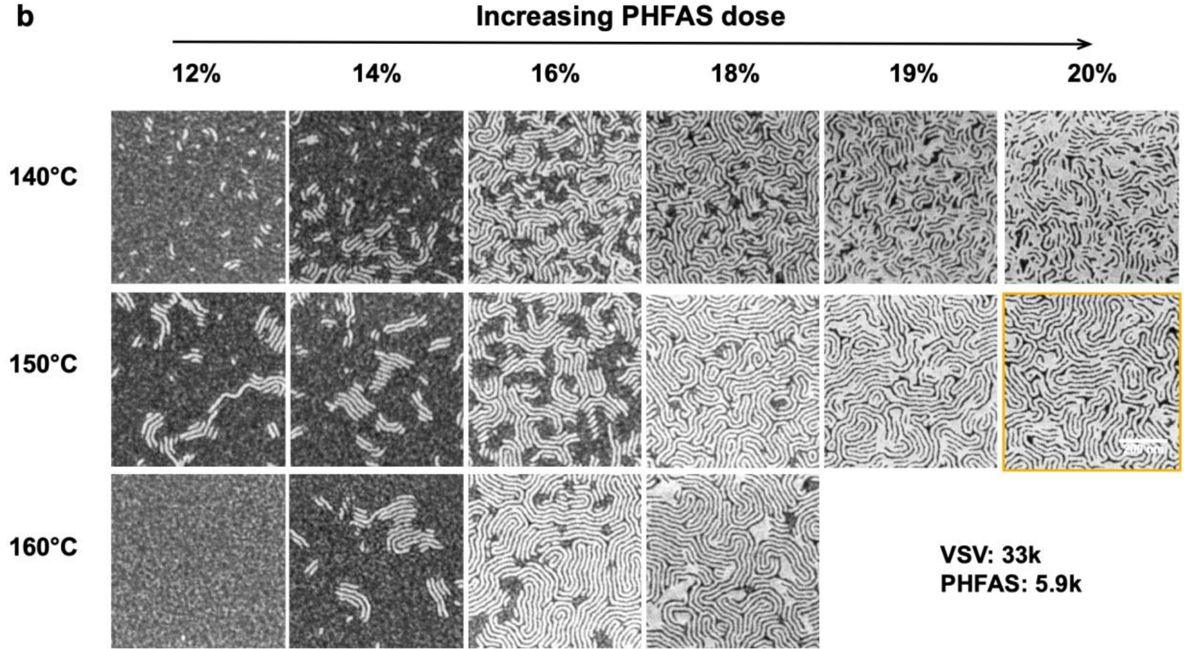

198 **Fig. 4** SEM images of 26k VSV and 33k VSV with various doses of 5.9k PHFAS upon thermal annealing on
199 neutral substrates. (a) For 26k VSV, full perpendicular orientation forms with 20% PHFAS at 150°C. (b) For 33k
200 VSV, no full perpendicular orientation can be observed. Scale bars represent 200 nm.

201 The PHFAS dose and annealing conditions were optimized for each VSV. For 26k and 33k
202 VSV, no meaningful results could be observed when mixed with 9.5k PHFAS. This is
203 presumably because the size of PHFAS needs to be similar as or smaller than the P2VP block
204 in order for it to interact effectively with the P2VP block, which is further supported by the
205 results when the VSV was mixed with smaller PHFAS. When 26k VSV was mixed with 5.9k
206 PHFAS (Fig. 4a), similar results were observed as that of 47k VSV mixed with 9.5k PHFAS.
207 Perpendicular orientation began to form as PHFAS dose increased, and full perpendicular
208 lamellae have been achieved with 20% PHFAS at 150°C. For 33k VSV, however, the self-
209 assembled pattern contained many defects after optimization, which could be potentially
210 attributed to the aggregation of PHFAS on top, since PHFAS is also amenable to SIS.
211 Alternatively, the defects could also possibly come from the parallel orientation of VSV with
212 P2VP on top. A more detailed study, such as transmission electron microscopy energy-
213 dispersive X-ray spectroscopy (TEM-EDX) would be required to determine the origin of the

214 defects, which could be investigated in the future work. Nevertheless, we have shown that these

215 defects could be eliminated by optimizing molecular weight of PHFAS.

216 **Table 1** Effect of molecular weight of PHFAS on orientation control.

M_{VSV} (g/mol)	M_{PHFAS} (g/mol)	M_{PHFAS}/M_{VSV}	Result
33k	5.9k	**0.18**	
47k	9.5k	**0.20**	
26k	5.9k	**0.23**	
33k	9.5k	**0.29**	

217

218 For a more quantitative analysis, we further calculate the ratio of molecular weight of PHFAS

219 (M_{PHFAS}) to the molecular weight of VSV (M_{VSV}), and compare it with the optimized

220 orientation control results as summarized in Table 1. When the ratio is 0.18, after optimizing

221 PHFAS dose and annealing conditions, perpendicular orientation can be observed, however

222 the optimized result still shows defective areas. As the M_{PHFAS}/M_{VSV} ratio increases, orientation

223 control also improves and fully perpendicular lamellae can be achieved. When the ratio is too

224 high, however, no perpendicular orientation can be observed. Consequently, the orientation is

225 best controlled when the ratio is between 0.20 and 0.23, which can provide us a preliminary

226 prediction of the PHFAS size needed for a given VSV.

227

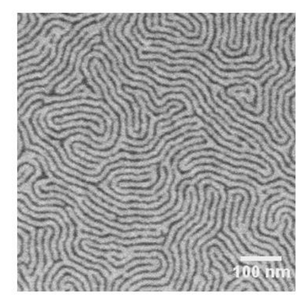

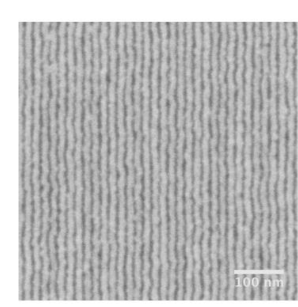

228 **Fig. 5** SEM images of (a) self-assembled VSV on neutral substrate and (b) DSA pattern with 5× density
229 multiplication. L_0 is 17.0 nm as measured by FFT analysis.

230 Among all the combinations, the VSV/PHFAS pair we chose for sub-10 nm patterning is 26k
231 VSV mixed with 20% 5.9k PHFAS (Fig. 5a). L_0 is 17.0 nm as measured from FFT analysis.
232 Following the same chemo-epitaxy DSA flow, we achieved 5 times density multiplication on
233 chemical patterns comprising of xPS guiding stripes and neutral brush (Fig.5b). This confirms
234 that our strategy applies to VSV with various molecular weights and periodicities, and therefore
235 can be an effective solution to sub-10 nm patterning.

236 ## 4 Conclusions

237 In this study, we have demonstrated that PHFAS can effectively balance the surface energies
238 of PS and P2VP blocks, and enable perpendicular orientation of VSV upon simple thermal
239 annealing. After optimizing PHFAS dose and annealing temperatures, we were able to achieve
240 full perpendicular orientation of VSV with L_0 as small as 17 nm. Successful chemo-epitaxy
241 DSA with density multiplication was demonstrated, and pattern transfer potential of this
242 material system has been revealed. We also investigated the relationship between molecular
243 weight of PHFAS and that of VSV, and provided a preliminary prediction of the PHFAS size
244 needed for a given VSV for optimal orientation control. This approach offers an effective
245 solution for sub-10 nm patterning with simple thermal annealing, and can be potentially
246 generalized to other high-χ BCPs as well.

247 ## 5 Acknowledgements

248 This work was primarily supported by National Science Foundation (Award No. 1344891).
249 This research used resources at the Center for Nanoscale Materials, a U.S. Department of
250 Energy Office of Science user facility operated by Argonne National Laboratory under
251 Contract No. DE-AC02-06CH11357. The authors are grateful for the support from the NSF
252 Materials Research Science & Engineering Center (MRSEC), Pritzker Nanofabrication
253 Facility and Searle Cleanroom in the University of Chicago. This work was previously
254 presented at SPIE Advanced Lithography[18].

255 **6 References**

256 [1] Kim, S. O., Solak, H. H., Stoykovich, M. P., Ferrier, N. J., De Pablo, J. J. and Nealey,
257 P. F., "Epitaxial self-assembly of block copolymers on lithographically defined
258 nanopatterned substrates," Nature **424**(6947), 411–414 (2003).

259 [2] Ruiz, R., Kang, H., Detcheverry, F. A., Dobisz, E., Kercher, D. S., Albrecht, T. R., De
260 Pablo, J. J. and Nealey, P. F., "Density multiplication and improved lithography by
261 directed block copolymer assembly," Science **321**(5891), 936–939 (2008).

262 [3] Gronheid, R., Rincon Delgadillo, P., Pathangi, H., Van den Heuvel, D., Parnell, D.,
263 Chan, B. T., Lee, Y.-T., Van Look, L., Cao, Y., Her, Y., Lin, G., Harukawa, R.,
264 Nagaswami, V., D'Urzo, L., Somervell, M. and Nealey, P., "Defect reduction and
265 defect stability in IMEC's 14nm half-pitch chemo-epitaxy DSA flow," Proc. SPIE
266 **9049**, 904905 (2014).

267 [4] Gu, X., Gunkel, I. and Russell, T. P., "Pattern transfer using block copolymers,"
268 Philos. Trans. R. Soc. A Math. Phys. Eng. Sci. **371**(2000), 20120306–20120306
269 (2013).

270 [5] Sauer, B. B. and Dee, G. T., "Surface tension and melt cohesive energy density of

271 polymer melts including high melting and high glass transition polymers," Macromolecules **35**(18), 7024–7030 (2002).
272

273 [6] Mark, J. E., [Physical Properties of Polymers Handbook] Springer, New York, 1012-
274 1018 (2007).

275 [7] Xiong, S., Wan, L., Ishida, Y., Chapuis, Y. A., Craig, G. S. W., Ruiz, R. and Nealey,
276 P. F., "Directed Self-Assembly of Triblock Copolymer on Chemical Patterns for Sub-
277 10-nm Nanofabrication via Solvent Annealing," ACS Nano **10**(8), 7855–7865 (2016).

278 [8] Suh, H. S., Kim, D. H., Moni, P., Xiong, S., Ocola, L. E., Zaluzec, N. J., Gleason, K.
279 K. and Nealey, P. F., "Sub-10-nm patterning via directed self-assembly of block
280 copolymer films with a vapour-phase deposited topcoat," Nat. Nanotechnol. **12**(6),
281 575–581 (2017).

282 [9] Zhang, J., Clark, M. B., Wu, C., Li, M., Trefonas, P. and Hustad, P. D., "Orientation
283 Control in Thin Films of a High-χ Block Copolymer with a Surface Active Embedded
284 Neutral Layer," Nano Lett. **16**(1), 728–735 (2016).

285 [10] Vora, A., Schmidt, K., Alva, G., Arellano, N., Magbitang, T., Chunder, A., Thompson,
286 L. E., Lofano, E., Pitera, J. W., Cheng, J. Y. and Sanders, D. P., "Orientation Control
287 of Block Copolymers Using Surface Active, Phase-Preferential Additives," ACS Appl.
288 Mater. Interfaces **8**(43), 29808–29817 (2016).

289 [11] Ji, S., Liu, C.-C., Son, J. G., Gotrik, K., Craig, G. S. W., Gopalan, P., Himpsel, F. J.,
290 Char, K. and Nealey, P. F., "Generalization of the Use of Random Copolymers To
291 Control the Wetting Behavior of Block Copolymer Films," Macromolecules **41**(23),
292 9098–9103 (2008).

293 [12] Liu, C.-C., Han, E., Onses, M. S., Thode, C. J., Ji, S., Gopalan, P. and Nealey, P. F.,
294 "Fabrication of Lithographically Defined Chemically Patterned Polymer Brushes and
295 Mats," Macromolecules **44**(7), 1876–1885 (2011).

296 [13] Delgadillo, P. A. R., Gronheid, R., Thode, C. J., Wu, H., Cao, Y., Neisser, M.,
297 Somervell, M., Nafus, K. and Nealey, P. F., "Implementation of a chemo-epitaxy flow
298 for directed self-assembly on 300-mm wafer processing equipment," J.
299 Micro/Nanolithography, MEMS, MOEMS **11**(3), 031302 (2012).

300 [14] Sun, Z., Chen, Z., Zhang, W., Choi, J., Huang, C., Jeong, G., Coughlin, E. B., Hsu, Y.,
301 Yang, X., Lee, K. Y., Kuo, D. S., Xiao, S. and Russell, T. P., "Directed Self-Assembly
302 of Poly(2-vinylpyridine)-b-polystyrene-b-poly(2-vinylpyridine) Triblock Copolymer
303 with Sub-15 nm Spacing Line Patterns Using a Nanoimprinted Photoresist Template,"
304 Adv. Mater. **27**(29), 4364–4370 (2015).

305 [15] Matsushita, Y., Mori, K., Saguchi, R., Nakao, Y., Noda, I. and Nagasawa, M.,
306 "Molecular weight dependence of lamellar domain spacing of diblock copolymers in
307 bulk," Macromolecules **23**(19), 4313–4316 (1990).

308 [16] Liu, C. C., Ramírez-Hernández, A., Han, E., Craig, G. S. W., Tada, Y., Yoshida, H.,
309 Kang, H., Ji, S., Gopalan, P., De Pablo, J. J. and Nealey, P. F., "Chemical patterns for
310 directed self-assembly of lamellae-forming block copolymers with density
311 multiplication of features," Macromolecules **46**(4), 1415–1424 (2013).

312 [17] Tseng, Y. C., Peng, Q., Ocola, L. E., Elam, J. W. and Darling, S. B., "Enhanced block
313 copolymer lithography using sequential infiltration synthesis," J. Phys. Chem. C
314 **115**(36), 17725–17729 (2011).

315 [18] Li, J., Zhou, C., Chen, X., Rincon-Delgadillo, P. A. and Nealey, P. F., "Directed self-

316 assembly of triblock copolymers for sub-10 nm nanofabrication using polymeric

317 additives," Proc. SPIE **10586**, 105860V (2018).

318